

Red Electrophosphorescence from a Soluble Binaphthol Derivative as Host and Iridium Complex as Guest

Xiong Gong,* Hadjar Benmansour, Guillermo C. Bazan,* and Alan J. Heeger

Institute for Polymers and Organic Solids, University of California, Santa Barbara, Santa Barbara, California 93106

Received: January 20, 2006; In Final Form: February 24, 2006

The investigation of the optical properties, carrier injection, and transport into a soluble small molecule, 6,6'-dicarbazolyl-2,2'-dihexyloxy-1,1'-binaphthol (BA), was reported. The results demonstrated that BA is a blue-emitting molecule, which can be used as a host for the fabrication of electrophosphorescent light-emitting diodes (LEDs). The single-layer electrophosphorescent LEDs fabricated from toluene solution containing BA with tris[2,5-bis-2'-(9',9'-dihexylfluorene)pyridine- κ^2 NC₃]iridium(III) [Ir(HFP)₃] emitted red light from Ir(HFP)₃ triplet emission. The results from photoluminescence (PL) and electroluminescence (EL) demonstrated that the dominated operational mechanism in EL was charge trapping rather than Förster transfer, which was the dominated mechanism in PL. The single-layer OLEDs with 1wt % of Ir(HFP)₃ have a luminance (*L*) of 1000 cd/m² at 22 V and a luminous efficiency (*LE*) of 0.88 cd/A at 11 mA/cm². Double-layer electrophosphorescent LEDs fabricated by casting the emitting layer from a solution of BA blended with Ir(HFP)₃ and subsequently thermally depositing tris(8-hydroxyquinoline) aluminum (Alq₃) film as an electron injection and transport layer yielded *L* = 1830 cd/m² at 30 V and *LE* = 2.47 cd/A at 18 mA/cm². These results demonstrated that electrophosphorescent LEDs can be fabricated from BA via solution processing and that *L* and *LE* can be enhanced by changing the device architecture with the goal of better balancing the electron and hole currents.

Introduction

Organic and polymeric light-emitting diodes (OLEDs and PLEDs) have received attention during the past decade because of potential applications in flat panel displays. They exhibit high brightness and efficiency, they operate at relatively low drive voltages, they emit a variety of colors, and they offer relatively simple fabrication.^{1–3} The performance of OLEDs and PLEDs has been dramatically improved by utilizing triplet emitters, that is, organometallic complexes, as dopants.^{4–6} For full color display applications, the achievement of three primary colors, red, green, and blue, with high efficiency and luminance at comparable drive voltages is essential.^{7,8} The blue emitters that are currently available have limited lifetimes.^{9,10} In addition, the red emitters have relatively low efficiency as compared to green emitters. Thus, there is ongoing effort directed toward small molecule and/or conjugated polymer systems that show efficient, stable blue and red emission.

Blue-emitting binaphthol cores have been demonstrated to be a suitable platform for the design of amorphous organic chromophores.^{11,12} They also provide sites with well-established substitution chemistry and an obvious practical advantage: as small molecules, they can be purified by standard organic techniques. Additionally, it is of interest to develop binaphthol derivatives with good solubility because it is promising to be less expensive to fabricate OLEDs using soluble small molecules by solution process than the traditional ones by vacuum deposition technology.

For OLEDs and PLEDs, an amorphous material with high *T_g* is desired;¹³ high *T_g* films are of considerable importance,

because the thermal and morphological stability of the deposited films influences the lifetime and performance of OLEDs.¹⁴ Binaphthol derivatives with a higher glass transition temperature (*T_g*) that emit from blue to green can be achieved by chemical substitution.^{12,15}

An additional incentive for the design of useful and durable blue-emissive materials originates from the fact that green and red emission can be obtained by doping a blue-emitting host material.^{4,6} Binaphthol derivatives with good solubility can be obtained by modification with alkoxy substituents.¹² This provides the benefit of precise control of the dopants at any ratio from a mother solution, provided that no phase separation occurs in the bulk. Solution-based processes also offer the advantage of low cost manufacturing by such techniques as ink-jet printing.

In this study, we investigated the optical properties, carrier injection, and transport into 6,6'-dicarbazolyl-2,2'-dihexyloxy-1,1'-binaphthol (BA). The results demonstrated that BA is a blue-emitting molecule that can be used as a host for the fabrication of electrophosphorescent light-emitting diodes (LEDs). The single-layer electrophosphorescent LEDs fabricated from toluene solution containing BA with tris[2,5-bis-2'-(9',9'-dihexylfluorene)pyridine- κ^2 NC₃]iridium(III) [Ir(HFP)₃] emitted red light from Ir(HFP)₃ triplet. The results from photoluminescence (PL) and electroluminescence (EL) demonstrated that the dominated operational mechanism in EL was charge trapping rather than Förster transfer, which was the dominated mechanism in PL. The single-layer OLEDs with 1wt % of Ir(HFP)₃ have a luminance (*L*) of 1000 cd/m² at 22 V and a luminous efficiency (*LE*) of 0.88 cd/A at 11 mA/cm². Double-layer electrophosphorescent LEDs made by BA blended with Ir(HFP)₃ as an emissive layer and tris(8-hydroxyquinoline) aluminum

* Corresponding authors. Fax: (805) 893-4755 (X.G.); (805) 893-4755 (G.C.B.). E-mail: xgong@physics.ucsb.edu (X.G.); bazan@chem.ucsb.edu (G.C.B.).

(Alq₃) as an electron-transporting layer emit red light with a $L = 1830 \text{ cd/m}^2$ at 30 V and $LE = 2.47 \text{ cd/A}$ at $J = 18 \text{ mA/cm}^2$.

Experimental Section

The 6,6'-dibromo-2,2'-dihexyloxy-1,1'-binaphthol was prepared according to previously reported procedures.^{11,12} A hexyl chain was introduced at the 2 and 2' positions to ensure good solubility. The carbazole unit was introduced at the 6 and 6' positions using the Buchwald–Hartwig cross coupling.^{13–16} 6,6'-dibromo-2,2'-dihexyloxy-1,1'-binaphthol was reacted with excess carbazole in refluxing toluene using palladium acetate Pd(OAc)₂, tri-*tert*-butylphosphine P(*t*-Bu)₃ as the ligand, and potassium carbonate (K₂CO₃) as the base. Few column chromatography separations were necessary to recover the disubstituted BA from the crude mixture containing carbazole and the monosubstituted adduct.

The synthesis of Ir(HFP)₃ was reported elsewhere.¹⁷

For optical measurements, thin films of BA and Ir(HFP)₃ were prepared by spin-casting on quartz substrates from toluene and dichloroethane solution (10 mg/mL), respectively. All films had approximately the same thickness (for direct comparison of the absorption and emission intensities). The absorption spectra of films were measured on a Shimadzu UV-2401PC UV–vis recording spectrophotometer. PL spectra of films were measured on a Spex Fluoromax-2 spectrometer.

For device fabrication, we employed single-active-layer and double-active-layer configurations with poly(3,4-ethylene dioxythiophene):poly(styrene sulfonic acid) (PEDOT:PSS) on indium tin oxide (ITO) as the hole-injecting bilayer electrode. The devices configurations are (ITO)/PEDOT:PSS/BA:Ir-(HFP)₃/Ba/Al and (ITO)/PEDOT:PSS/BA:Ir(HFP)₃/Alq₃/Ba/Al. PEDOT:PSS was first spun-cast onto ITO surface, and then the emitting layer was spun-cast to a film with thickness of approximately 100 nm. An approximately 30 nm of tris(8-hydroxyquinoline) aluminum (Alq₃) was subsequently thermally deposited on the top of the emitting layer. The Ba/Al cathode was deposited through a shadow mask by thermal evaporation at 4×10^{-7} Torr.

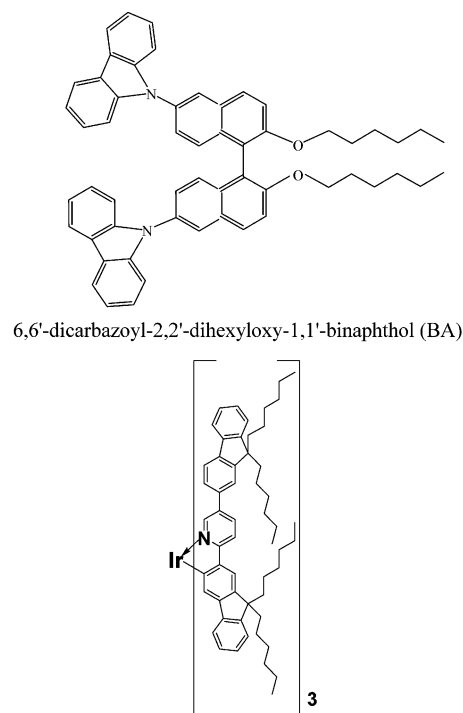
Device performance was measured inside of the drybox. The current–voltage–luminance characteristics were measured using a Keithley 236 source measurement unit. The EL spectra were measured using an Oriel Ocean CCD spectrograph. The luminance was obtained in forward viewing direction (detector subtended 0.01 sr solid angle) using a calibrated silicon photodiode.^{6,18} The luminous efficiency was converted from measured luminance.^{6,18}

Results and Discussion

The molecular structures of BA and Ir(HFP)₃ are shown in Scheme 1. The new soluble host BA based on the binaphthol framework contains the well-known carbazole unit, which will provide good charge mobility and a low barrier to injection. The T_g of BA is 171 °C, as determined by DSC and DTA measurements. A high T_g of BA indicated that BA thin film has good thermal and morphological stability. As a result, the OLEDs fabricated by BA will have a long-lifetime and high-performance because the thermal and morphological stability of the films play an important role in the performance of OLEDs.¹⁹

To investigate the charge injection into and transport in BA, “electron-only” and “hole-only” devices were fabricated with the following structures: Yb/BA/Ba/Al and ITO/BA/Au.^{8,20,21} Because of the low work functions of the metals used for the electrodes in the “electron-only” devices (Yb and Al) and the

SCHEME 1: Molecular Structures of BA and Ir(HFP)₃



Tris[2,5-bis-2'-(9',9'-dihexylfluorene)pyridine- κ^2 NC₃]₃Iridium(III) [Ir(HFP)₃]

TABLE 1: Device Characteristics

Ir(HFP) ₃ /BA (wt %)	turn-on voltage (V)	LE @ 100 cd/m ² (cd/A)	LE _{max} (cd/A)	L _{max} (cd/m ²)
0.1	~5	0.21	0.32	460
0.2	~5	0.34	0.48	530
0.5	~5	0.46	0.67	820
1	~5	0.65	0.88	1000
5	~5	0.56	0.72	960

high work functions of the metals used for the electrodes in the “hole-only” devices (ITO and Au), holes are not injected into “electron-only” devices and electrons are not injected into “hole-only” devices.

Figure 1a shows the current density (J) versus applied voltages (V) for both “electron-only” and “hole-only” devices. The hole current density in the “hole-only” devices is an order of magnitude larger than the electron current density in the “electron-only” devices (at the same electric field). The larger hole current is consistent with the hole mobility being greater than the electron mobility, as is commonly found in organic semiconductors. Thus, these results demonstrated that the hole mobility is higher than the electron mobility in BA.

On the other hand, Figure 1a demonstrates that the current densities for both “hole-only” and “electron-only” devices are dependent on the electric field. Such field-dependent behavior is usually associated with tunneling processes.

Fowler–Nordheim tunneling theory predicts²²

$$I \propto F^2 \exp\left(\frac{-\kappa}{F}\right) \quad (1)$$

where I is the current, F is the electric-field strength, and κ is a parameter that depends on the barrier shape. Figure 1b shows a plot of $\ln(I/F^2)$ versus $1/F$ for both type of devices with a 200 nm thick BA layer. It can be seen that the plot approaches to be linear at the voltage of approximately 5 V, which is the turn-

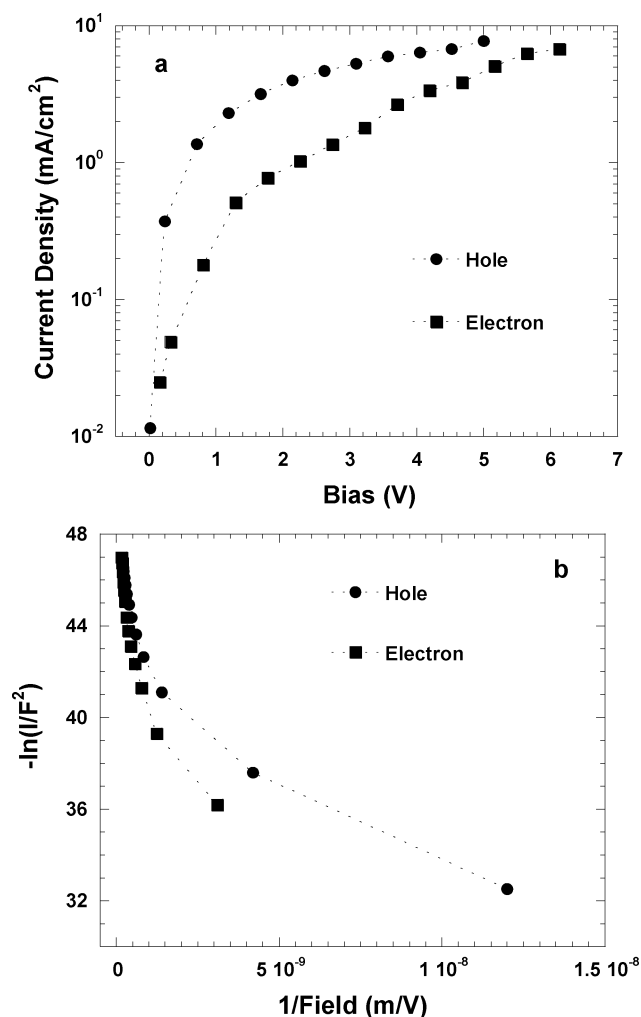


Figure 1. (a) The bias versus current density (V vs J) for devices made with BA; (b) Fowler–Nordheim plot for 200 nm thickness of BA for “electron-only” devices, Yb/BA/Ba/Al (■), and “hole-only” devices, ITO/BA/Au (●).

on voltage for the device made by BA (see Table 1). The deviation from linear at lower voltage is likely originated from a thermionic emission contribution to the current.²⁰

If the injected charge is tunneling through a triangular barrier at one of the polymer interfaces, the constant κ in eq 1 is given by

$$\kappa = \frac{8\pi\varphi^{3/2}\sqrt{2m^*}}{3q\hbar} \quad (2)$$

Here, φ is the barrier height, and m^* is the effective mass of the holes in BA. Assuming the effective mass equals the free electron mass and the electric field is constant across the BA layer, the calculated barrier heights for hole tunneling into “hole-only” and electron tunneling into “electron-only” devices are 0.3–0.6 and 0.4–0.7 eV, respectively. These results indicated that the hole injection into BA from ITO electrode is easier than the electron injection into BA from Ba electrode.

The absorption and photoluminescence (PL) spectra of the BA thin films are shown in Figure 2. The absorption spectrum of BA shows the characteristic vibronic structure of carbazole.¹¹ BA emits in the blue region of the spectrum. The absorption and PL spectra of Ir(HFP)₃ thin films are also shown in Figure 2. Ir(HFP)₃ emits in the red region of the spectrum.^{20,21} The emission spectrum of BA overlaps with the metal–ligand-charge-transfer (MLCT) absorption band of Ir(HFP)₃, implying

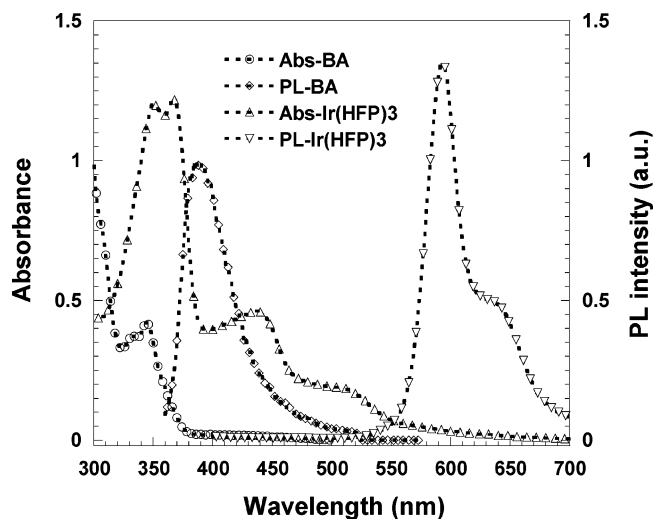


Figure 2. Absorption and photoluminescence spectra of BA and Ir(HFP)₃ thin films.

an efficient Förster transfer from BA to the MLCT band of Ir(HFP)₃ is expected.^{4,6}

To test the efficiency of energy transfer, thin films of BA with different concentrations of Ir(HFP)₃ were prepared and optically excited. The PL spectra of BA and BA with different concentrations of Ir(HFP)₃ excited at 350 nm are shown in Figure 3a. The PL profile contains two peaks: one centered at 395 nm, which results from the emission of BA host; and a second at 600 nm with a shoulder at 620 nm, which results from the Ir(HFP)₃ triplet emission. The emission intensity at 395 nm reduced significantly as the Ir(HFP)₃ concentration increased. At 5 wt % Ir(HFP)₃, the emission observed from BA is very weak and the emission from Ir(HFP)₃ completely dominated. Therefore, efficient Förster energy transfer from BA to Ir(HFP)₃ is confirmed by the dominant emission from the Ir(HFP)₃.^{23,24}

The EL spectra observed from the single layer electrophosphorescent LEDs at a current density of 2 mA/cm² were shown in Figure 3b. The single layer electrophosphorescent LEDs with a configuration of ITO/PEDOT:PSS/BA:Ir(HFP)₃/Ba/Al were fabricated by casting films comprising BA as host and different concentrations of Ir(HFP)₃ as guest. The EL spectra from any devices containing Ir(HFP)₃ only show the characteristic spectrum of Ir(HFP)₃, with one peak at 600 nm and another at 620 nm. There is no emission of BA from any devices containing Ir(HFP)₃, even at 0.1 wt % guest concentration. Note that the concentration of Ir(HFP)₃ required to completely quench the BA PL emission was larger than 5 wt %. The absence of BA EL emission from the devices containing the Ir(HFP)₃, even at the lowest concentration of Ir(HFP)₃ (0.1 wt %), is consistent with charge trapping on the Ir-complex (rather than Förster transfer) as the dominant mechanism in the LEDs. We conclude, therefore, that the iridium complex traps both electrons and holes, which enables the direct recombination of holes and electrons via the Ir-complex. If energy transfer were the dominant EL mechanism, the EL emission of BA would be expected to appear when the triplet of Ir(HFP)₃ becomes saturated, that is, at higher applied voltages and lower concentrations.^{25,26} Similar “charge trapping” has been observed in PVK-PBD doped with Ir-complexes,^{6,27–29} and in conjugated polymers doped with Ir-complexes.^{16,30}

Table 1 summarizes the devices characteristics. The devices turn-on occurs at approximately 5 V, that is, at significantly lower voltage than the typical turn-on voltage of devices made

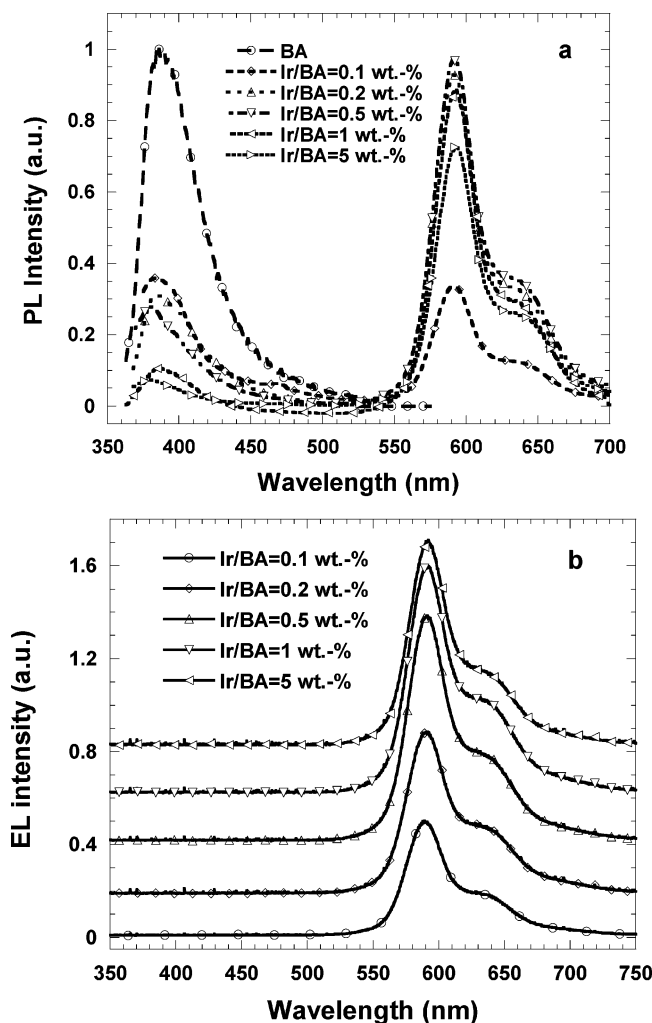


Figure 3. (a) The photoluminescence spectra of thin films made with BA and BA blended with different concentrations of Ir(HFP)₃ under the excitation of 340 nm; and (b) the electroluminescence spectra of the devices made with BA with different concentrations of Ir(HFP)₃ at current density of 2 mA/cm².

from small molecules,²⁹ but comparable to the turn-on voltage of devices made from PFO as the host.²⁴ Devices with 1 wt % of Ir(HFP)₃ exhibited $L \approx 1000$ cd/m² at 22 V with $LE = 0.88$ cd/A at $J = 11$ mA/cm². These devices parameters are comparable to that using conjugated polymers as the host,³⁰ but it is worse than that using PVK-PBD as the host.⁶ The poor device performance is due to the unbalanced charge carriers in BA, originating from certain barrier heights for both hole and electron injection, and BA is a hole-mobility dominated molecule (see Figure 1). The low PL quantum yield of BA also resulted in poor devices performance.^{2,12}

Because both the hole mobility and the hole injection are greater than the electron mobility and electron injection in BA (see Figure 1), the charge carriers are unbalanced in these BA-based devices. To enhance the electron injection and transport, double-layer OLEDs were fabricated by using Alq₃ as an electron-transporting layer (ETL). The device structure has the following architecture: (PEDOT:PSS) ITO/BA:Ir(HFP)₃/Alq₃/Ba/Al. The emitting-layer was deposited using the same solution process as that single-layer device. Alq₃ (~40 nm) was deposited by thermal evaporation.

The double-layer devices exhibited $L = 1830$ cd/m² at 30 V with $LE = 2.47$ cd/A at $J = 18$ mA/cm². The L and LE data as a function of J for double- and single-layer devices are shown

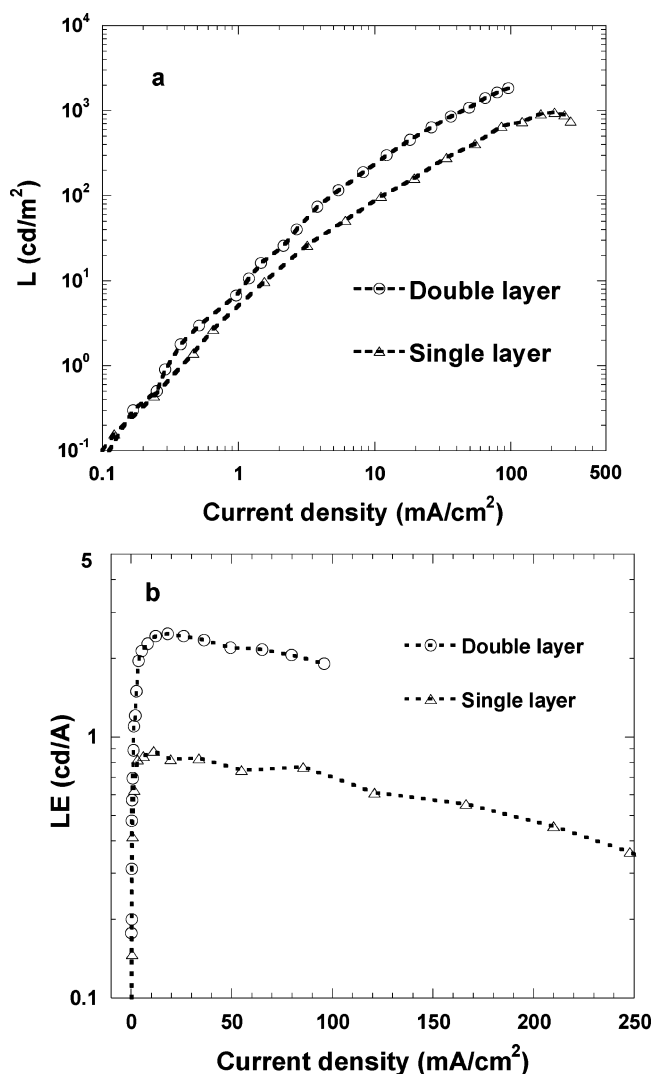


Figure 4. The L (a) and LE (b) as a function of J for double- (○) and single-layer (Δ) devices. Architecture for single-layer devices: (PEDOT:PSS)ITO/BA:Ir(HFP)₃/Ba/Al. Architecture for double-layer devices: (PEDOT:PSS)ITO/BA:Ir(HFP)₃/Alq₃/Ba/Al.

in Figure 4a and b, respectively. At the same J , the L and LE values for double-layer devices were much higher than those for single-layer devices. These demonstrated that L and LE could be increased by achieving better balance of the electron and hole currents by using Alq₃ as an ETL.

Conclusions

In conclusion, the investigation of the optical properties, carrier injection, and transport into BA demonstrated that this soluble blue-emitting binaphthol derivative could be used as an electroluminescent material. The results from PL and EL demonstrated that the dominated operational mechanism in EL was charge trapping rather than Förster transfer, which was the dominated mechanism in PL. The single-layer OLEDs with 1 wt % of Ir(HFP)₃ have a L of 1000 cd/m² at 22 V and a LE of 0.88 cd/A at 11 mA/cm². Double-layer electrophosphorescent LEDs fabricated using BA blended with Ir(HFP)₃ as an emitting layer and Alq₃ as an electron-transporting layer have $L = 1830$ cd/m² at 30 V and $LE = 2.47$ cd/A at 18 mA/cm². These results demonstrated that single-layer electrophosphorescent LEDs can be fabricated from the toluene solution containing BA with Ir(HFP)₃ and both L and LE could be increased by achieving better balance of the electron and hole currents by using Alq₃ as an ETL.

Acknowledgment. We thank Jacek C. Ostrowski at UCSB for synthesis of the Ir-complex. H.B. thanks Dr. Jacek Brezinski for the discussion on the synthesis of BA.

References and Notes

- (1) Burroughes, J. H.; Bradley, D. D. C.; Brown, A. R.; Marks, R. N.; Mackay, K.; Friend, R. H.; Burn, P. L.; Holmes, A. B. *Nature* **1990**, *347*, 539.
- (2) Gustafsson, G.; Cao, Y.; Treacy, G. M.; Klavetter, F.; Colaneri, N.; Heeger, A. J. *Nature* **1992**, *357*, 477.
- (3) Heeger, A. J. *Angew. Chem., Int. Ed.* **2001**, *40*, 2591.
- (4) McGehee, M. D.; Bergstedt, T.; Zhang, C.; Saab, A. P.; O'Regan, M. B.; Bazan, G. C.; Srdanov, V. I.; Heeger, A. J. *Adv. Mater.* **1999**, *11*, 1349.
- (5) Adachi, C.; Baldo, M. A.; Forrest, S. R. *Appl. Phys. Lett.* **2000**, *77*, 904.
- (6) Gong, X.; Ostrowski, J. C.; Robinson, M. R.; Moses, D.; Bazan, G. C.; Heeger, A. J. *Adv. Mater.* **2002**, *14*, 581.
- (7) Zhang, C.; Heeger, A. J. *J. Appl. Phys.* **1998**, *84*, 1579.
- (8) Gong, X.; Ma, W. L.; Ostrowski, J. C.; Moses, D.; Bazan, G. C.; Heeger, A. J. *Adv. Funct. Mater.* **2004**, *14*, 393.
- (9) Gong, X.; Iyer, P.; Moses, D.; Bazan, G. C.; Heeger, A. J. *Adv. Funct. Mater.* **2003**, *13*, 325.
- (10) Uckert, F.; Tak, Y. H.; Müllen, K.; Bäessler, H. *Adv. Mater.* **2000**, *2*, 905.
- (11) Ostrowski, J. C.; Hudack, R. A.; Robinson, M. R.; Wang, S. J.; Bazan, G. C. *Chem.-Eur. J.* **2001**, *7*, 4500.
- (12) Benmansour, H.; Shioya, T.; Sato, Y.; Bazan, G. C. *Adv. Funct. Mater.* **2003**, *13*, 883.
- (13) Buchwald, S.; Muci, A. *Top. Curr. Chem.* **2002**, *219*, 133.
- (14) Hartwig, J. *Pure Appl. Chem.* **1999**, *71*, 1417.
- (15) Buchwald, S.; Yang, B. *J. Organomet. Chem.* **1999**, *576*, 125.
- (16) Hartwig, J. *Acc. Chem. Res.* **1998**, *31*, 852.
- (17) Parker, I. D. *J. Appl. Phys.* **1994**, *75*, 1658.
- (18) Müllen, K., Ed. *Electroluminescence-from Synthesis to Devices*; Wiley-VCH: New York, 2006; p 151.
- (19) Kim, J. S.; Friend, R. H.; Cacialli, F. *Appl. Phys. Lett.* **1999**, *74*, 3084.
- (20) Ostrowski, J. C.; Robinson, M. R.; Heeger, A. J.; Bazan, G. C. *Chem. Commun.* **2002**, *7*, 784.
- (21) Gong, X.; Ostrowski, J. C.; Bazan, G. C.; Moses, D.; Heeger, A. J. *Appl. Phys. Lett.* **2002**, *11*, 3711.
- (22) Fowlwe, R. H.; Nordheim, L. *Proc. R. Soc. London, Ser. A* **1928**, *119*, 173.
- (23) Gong, X.; Lim, S. H.; Ostrowski, J. C.; Moses, D.; Bardeen, C. J.; Bazan, G. C. *J. Appl. Phys.* **2004**, *95*, 948.
- (24) Gong, X.; Ostrowski, J. C.; Bazan, G. C.; Moses, D.; Heeger, A. J. *J. Polym. Sci., Part B: Polym. Phys.* **2003**, *41*, 2691.
- (25) O'Brien, D. F.; Giebler, C.; Fletcher, R. B.; Cadlby, J.; Palilis, L. C.; Lidzey, D. G.; Lane, P. A.; Bradley, D. C.; Blau, W. *Synth. Met.* **2001**, *116*, 379.
- (26) Baldo, M. A.; Forrest, S. R. *Phys. Rev. B* **2000**, *62*, 10958; **2000**, *62*, 10967.
- (27) Lamansky, S.; Djurovich, P.; Murphy, D.; Abdel-Razzaq, F.; Lee, H. E.; Adachi, C.; Burrows, P. E.; Forrest, S. R.; Thompson, M. E. *J. Am. Chem. Soc.* **2001**, *123*, 4304.
- (28) Lamansky, S.; Kwong, R. C.; Nugent, M.; Djurovich, P. I.; Thompson, M. E. *Org. Electron.* **2001**, *2*, 53.
- (29) Sakuratani, Y.; Asai, M.; Sone, M.; Miyata, S. *J. Phys. D: Appl. Phys.* **2001**, *34*, 3492.
- (30) Gong, X.; Ostrowski, J. C.; Moses, D.; Bazan, G. C.; Heeger, A. J.; Liu, M. S.; Jen, A. K.-Y. *Adv. Mater.* **2003**, *15*, 45.